Chemical Engineering Journal 471 (2023) 144520

Contents lists available at ScienceDirect

Chemical Engineering Journal

journal homepage: www.elsevier.com/locate/cej

Removal of diclofenac by UV-B and UV-C light-emitting diodes (LEDs) driven advanced oxidation processes (AOPs): Wavelength dependence, kinetic modelling and energy consumption

Raffaella Pizzichetti [a,b,c], Ken Reynolds [b], Cristina Pablos [a,*], Cintia Casado [a], Eric Moore [c], Simon Stanley [b], Javier Marugán [a]

[a] Department of Chemical and Environmental Technology, ESCET, Universidad Rey Juan Carlos, C/Tulipán s/n, 28933 Móstoles, Madrid, Spain
[b] ProPhotonix IRL LTD, 3020 Euro Business Park, Little Island, Cork T45 X211, Ireland
[c] Environmental Research Institute, University College Cork, Lee Road, Cork T23 XE10, Ireland

ARTICLE INFO

Keywords:
Degradation kinetic
Photolysis
Free chlorine
Hydrogen peroxide
Dual-wavelength
Contaminants of emerging concern

ABSTRACT

In this study, the degradation of diclofenac (DCF), a frequently detected non-steroidal pharmaceutical, was evaluated by using UV-B and UV-C (265, 285, and 310 nm) light-emitting diodes (LEDs) alone and in combination with hydrogen peroxide (UV/H_2O_2) and free chlorine (UV/FC). The degradation of DCF followed a pseudo first-order kinetic, and their trend reflected the pattern of the molar absorption coefficients of the DCF and the oxidants. A positive synergistic factor was found for the UV-LED driven advanced oxidation processes in almost all cases, but despite the higher degradation rates, the overall electricity demand is similar to UV alone due to the oxidants' energy cost. The rigorous kinetic degradation mechanisms at different wavelengths were proposed for the two processes, UV/H_2O_2 and UV/FC, where the predicted values were respectively $k_{HO} = 9.12 \cdot 10^9\ M^{-1}\ s^{-1}$ and $k_{Cl} = 1.30 \cdot 10^{10}\ M^{-1}\ s^{-1}$. No significant synergy ($p > 0.05$) was found for the dual-wavelength system (265 + 285 nm), and the time-based constants in all cases changed linearly with lamp intensity. Finally, dissolved organic carbon and phytotoxicity analysis revealed low mineralisation (around 20–30%) associated with the formation of stable dimers and a decrease in toxicity towards tomato and radish seeds. In the main, this work shows the great potential of implementing wavelength-specific LEDs in water treatments and effectively designing the reactor playing with adjustable intensities and kinetic degradation rates.

1. Introduction

Safe water is an essential resource for life, yet contaminants of emerging concern (CECs) are an increasing threat to global health and require immediate action. Among others, CECs include pharmaceuticals, personal care products, flame retardants, pesticides, and endocrine disruptors. Their presence in the environment is not necessarily new, but the worries about their possible consequences are due to their potential associated risks to ecosystems and human beings [1]. Conventional treatments and natural attenuation are not enough to remove these pollutants from waste, surface, and drinking water and therefore, they are destined to bioaccumulate in aquatic ecosystems and human bodies [2]. Furthermore, CECs are poorly documented and are not controlled by standardised legislation, thus, increasing their exposure risk [1].

Abbreviations: AOP, Advanced oxidation process; CEC, Contaminant of emerging concern; DCF, Diclofenac; DOC, Dissolved organic carbon; EEO, Electric energy per order; FC, Free chlorine; GI, Germination Index; HPLC, High-performance liquid chromatography; LED, Light-emitting diode; LOD, Limit of detection; LOQ, Limit of quantification; MSSA, Micro steady state approximation; NRMSE, Normal root mean squared error; PMS, Peroxymonosulfate; PS, Persulfate; SQP, Sequential quadratic programming; A, Absorbance value; V_R, Active volume of the reactor; C, Concentration; L_C, Control roots length; G_C, Control seeds germination; Eq, Equivalent electric energy consumption; G_λ, Incident radiation; P, Lamp power input; ε_λ, Molar absorption coefficient; b, Path lengths; Φ_λ, Quantum yield; L_S, Sample roots length; G_S, Sample seeds germination; p, Significance level; F_S, Synergy factor; t, Time; k, Time-based kinetic constant; V_T, Total volume of the reactor; k', UV fluence-based kinetic constant; *VRPA*, Volumetric rate of photon absorption.

* Corresponding author.
E-mail addresses: raffaella.pizzichetti@urjc.es, rpizzichetti@prophotonix.com (R. Pizzichetti), kreynolds@prophotonix.com (K. Reynolds), cristina.pablos@urjc.es (C. Pablos), cintia.casado@urjc.es (C. Casado), 121116712@umail.ucc.ie, e.moore@ucc.ie (E. Moore), sstanley@prophotonix.com (S. Stanley), javier.marugan@urjc.es (J. Marugán).

https://doi.org/10.1016/j.cej.2023.144520
Received 31 March 2023; Received in revised form 14 June 2023; Accepted 29 June 2023
Available online 1 July 2023
1385-8947/© 2023 The Author(s). Published by Elsevier B.V. This is an open access article under the CC BY-NC license (http://creativecommons.org/licenses/by-nc/4.0/).

Also, considering the continuing increase in anthropogenic pollution, such as the intensification of pharmaceuticals or plastic additives usage, and the occurrence of natural disasters due to climate change, the available water quality is reducing, and therefore it is essential to develop strategies to increase our water resilience and prevent and reduce the CECs incidence. Among the technologies available to remove these micropollutants, UV radiation-driven advanced oxidation processes (AOPs), which exploit the generation of highly reactive radicals using UV light, is considered one of the most effective emerging technologies for environmental remediation [3,4]. However, a significant drawback of this technology is the use of medium-pressure or low-pressure mercury lamps since they are fragile, oversized, and contain mercury, which is hazardous for the environment and human health and requires a proper disposal protocol [5]. Therefore, a major contribution to UV treatments can be made by the advances in light-emitting diodes (LEDs) in the UV-B and UV-C range. They provide a mercury-free solution other than high design flexibility, tuneable wavelength, and instant on–off. For the AOPs choice, a recent study conducted by Pesqueira et al. [6] assessed the life cycle impacts of UV-C combined with hydrogen peroxide (H_2O_2), peroxymonosulfate (PMS), and persulfate (PS), and it revealed that H_2O_2 was the best environmental choice. On the other hand, UV/free chlorine (FC) is an emerging AOP that has become increasingly popular thanks to its low cost and since chlorine is already used in water as a disinfection agent against re-contamination [7,8]. In addition to hydroxyl radicals ($HO^{\bullet}$), UV/FC process produces reactive chlorine species (RCS) active in the degradation of the pollutants [8,9]. The photolysis of the contaminants, hydrogen peroxide, and chlorine is wavelength dependent, and therefore a compromise between the most effective wavelength and the overall highest removal efficiency should be found [10]. For hydrogen peroxide, the shortest wavelength has the highest degradation efficiency and photon absorption. Whereas HOCl and OCl^- have their peak absorption respectively at 235 and 292 nm [11,12].

Therefore, this study aims to evaluate the efficiency of UV alone, UV/H_2O_2 and UV/FC treatment by means of UV-B and UV-C (265, 285 and 310 nm) LEDs by tuning the working wavelength to optimise the contaminant and the oxidant absorption. Among the CECs, diclofenac (DCF), a non-steroidal anti-inflammatory drug, was selected for the study since it has been added to the first EU *watch list* under the Environmental Quality Standards Directive, and it has been detected up to μg L^{-1} in water bodies [13–15]. The experimental data were used to model the DCF kinetic degradation mechanisms based on the wavelength and the oxidation process. Furthermore, considering the unique characteristics of the UV-LEDs, the two most efficient lamps were studied under different lamp intensities and combined to evaluate the effectiveness of dual-wavelength UV photolysis. Indeed, the latter has not been significantly investigated for the degradation of the contaminants, but it is argued that it could lead to interesting outcomes [16]. The electrical energy consumption was evaluated in all cases to analyse the most efficient solution. Changes in dissolved organic carbon (DOC) as well as a phytotoxicity test of the diclofenac and the by-products after treatment, were measured and evaluated. On the other hand, assessing the effects of varying initial diclofenac concentration, pH, presence of scavengers and other organic matter, or increase of the oxidant dosage was out of the scope of this work since already been covered in other studies [17–20].

2. Materials and methods

2.1. Chemicals and materials

Sodium diclofenac (>99%), acetonitrile (HPLC grade), sodium hypochlorite solution (6–14% active chlorine), sodium thiosulfate reagent plus 99%, hydrogen peroxide solution 30% (w/w), titanyl sulfate solution, sodium sulfate, sulfuric acid 96%, sodium acetate, ferric sulfate pentahydrate, iron (II) sulfate heptahydrate, oxalic acid dihydrate, and 1,10 phenanthroline were all purchased by Merck, Sigma Aldrich. Finally, a Milli-Q water system supplied distilled water and deionised water employed during the study.

2.2. Photoreactor setup

The experiments were performed in a recirculating photoreactor system, shown in Fig. 1. The reactor included a resistant plastic container of 4 L (Nalgene® round carboy with spigot, Merck), a pressure transmitter (DRTR-ED-20MA, Automation24), a flow rate sensor (YF-S201, Botnroll), and a centrifugal pump (NDP14/2, Xylem Flojet) to recirculate the content, connected to a variable-frequency drive (AC10, Parker) to regulate its power. The sensors were directly connected to an Arduino Mega 2560 board integrated with a keypad, an LCD monitor, and an SD memory card to read and save the data instantaneously. Finally, a PID controller was implemented in the Arduino code (freely available in the GitHub repository) to work at a constant flow rate of 1 L min^{-1}. The photoreactor consisted of a quartz tube of 20 mm in inner diameter and 270 mm in length, where the LED lamps (COBRA Clean FX1, ProPhotonix IRL) were positioned at around 2 mm from the outer diameter of the quartz tube. Three lamps were employed during the study emitting according to their data sheets at 265, 285 and 310 nm. They consisted of sixteen LEDs built into compact and fan-cooled devices that provide a stable light emission over time without significant changes in the temperature.

Chemical ferrioxalate actinometry experiments were then carried out as described in the literature to calculate the total irradiation power of the lamps in the system when the water was recirculating [21]. Ferrioxalate actinometry was chosen over other experiments for its high reproducibility and the economic and environmental sustainability of the materials. The intensity and the spectra of the UV LED lamps were also measured by an ILT spectroradiometer (2003357U1, ILT), which proved to work well in the UV range considered [22]. It is worth mentioning that the area considered in the chemical actinometry corresponds to the part of the plane crossing the middle of the quartz tube irradiated from the lamps (108 mm · 20 mm). On the other hand, the radiometer was measured at 13.5 mm away, which was the distance from the mentioned plate to the light source; further details can be found in Appendix A and B of the Supplementary Information. Finally, the DCF solution was prepared directly in distilled water in order to avoid biases due to the presence of an organic solvent, which could be a competitor in the reactions with the radicals, influencing the final result [23].

2.3. Analytical methods

The detection and quantification of sodium diclofenac were conducted through high-performance liquid chromatography (HPLC) with a reverse C18 column and equipped with a diode detector (1200 Series, Agilent Technology). The optimised mobile phase was acetonitrile and 25 mM phosphate acetate buffer (pH 3) in a ratio of 80:20 v/v. The flow was set to 1 mL min^{-1} and the injection volume to 5 μL. Finally, the pressure was constant at 45 bar, the thermostat at 25 °C, and the detection wavelength was set at 210 nm. The samples for the calibration were prepared in half water and half mobile phase to best represent the sample from the experiments, which were diluted 1:1 with the mobile phase before quantification. DCF calibration is shown in Appendix C, and the method was validated in terms of specificity, linearity, precision, and accuracy. The limit of detection (LOD) and quantification (LOQ) were found to be 0.25 and 1 μg mL^{-1}, respectively.

The concentrations of free chlorine in the sample treated with UV/FC were determined using the Hanna Instrument kit with the portable photometer (HI97734, Hanna Instrument) and the corresponding reagents (HI93734, Hanna Instrument). Because of the upper limit of 10 mg L^{-1}, the sample was diluted before the measurement with deionised water when higher concentrations were expected. The method was more extensively reported in Appendix D of the Supplementary Information.

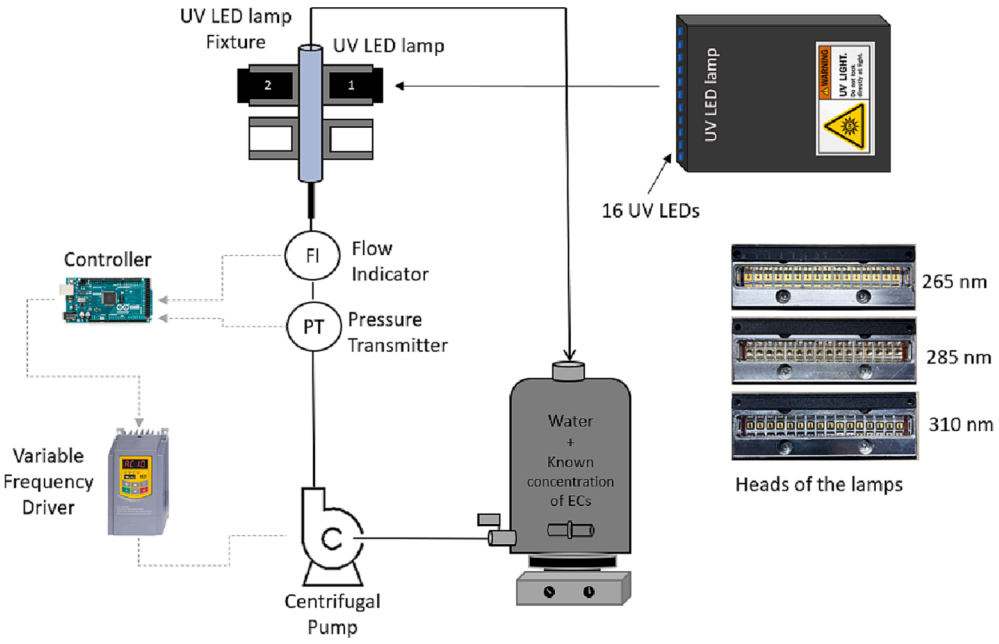

Fig. 1. UV-B and UV-C LED photoreactor working in recirculation to evaluate DCF degradation through LED-driven AOPs.

To evaluate the concentration of hydrogen peroxide in the UV/H_2O_2 process, titanyl sulfate solution was employed to form yellow complexes detectable at 410 nm. The calibration line, together with the method details, are reported in Appendix E of the Supplementary Information.

The absorptions of the solutions at different wavelengths were evaluated through a spectrophotometer working in the visible light, in the range 400–800 nm (V-3000PC, VWR), and with a UV–Vis spectrophotometer (8453, Agilent) for evaluations at a shorter UV range, 200–400 nm.

Finally, DOC removal was measured after filtrating the sample solution to separate any potential particulate organic carbon with a TOC-VCPH analyser (Shimadzu), where the method described in the TOC-V CPH/CPN Total Organic Carbon Analyser User's Manual was followed.

2.4. Phytotoxicity test

As described in the work of Ghanbari et al. [24], the germination index (GI) was used to evaluate the phytotoxicity of the treated DCF samples. In our experiment, fifteen seeds of each plant, *Raphanus sativus* (radish) and *Solanum Lycopersicum* (tomato), were distributed homogenously in the Petri dish containing one filter paper of 110 mm at the bottom and one filter paper of 70 mm on top of the wet seeds (Whatman, GE Healthcare Life Sciences). Distilled water was used for the control tests, and 10 mL of sample was used in each experiment. After incubating for 72 h at 25 °C, the number of germinated seeds was measured (G_S), as well as the length of the roots (L_S), and then compared to the germinated seeds in the control condition (G_C, and L_C, respectively). Finally, the GI was calculated following Eq. (1). The results show the average and the deviation standard of three repetitions for each sample.

$$GI(\%) = \frac{G_s \cdot L_s}{G_c \cdot L_c} \cdot 100 \tag{1}$$

2.5. Kinetic model derivation

The kinetic model was derived by resolving the mass balance of the different species and by applying the kinetic micro steady state approximation (MSSA) for the concentration of radicals. The kinetic parameters to estimate were calculated by minimising the normal root mean squared error (NRMSE) between the experimental and predicted concentration of DCF, H_2O_2, and FC. The sequential quadratic programming (SQP) function was then implemented in GNU Octave to solve the nonlinear optimisation and minimise the objective error function, whereas the system of differential equations was solved using Euler explicit method.

The rates of the elementary photoactivated reactions for H_2O_2, HOCl, and OCl^- photolysis were simplistically expressed as the product of the quantum yield of the reaction (Φ_λ, dimensionless but can be expressed in mol Einstein^{-1} considering that one Einstein is equal to one mol of photons) and the volumetric rate of photon absorption, *VRPA* (e^a, expressed in Einstein L^{-1} s^{-1}). Where the latter can also be written as the molar absorption coefficient of the reactant (ε_λ, M^{-1} cm^{-1}) multiplied by the concentration of the reactant and the irradiance (G_λ, W m^{-2}), Eq (2) [25]. Each value is wavelength dependent and therefore evaluated for each lamp.

$$A \xrightarrow{h\nu} B \qquad r_{A,\lambda} = \Phi_{A,\lambda} \cdot e^a{}_{A,\lambda} = \Phi_{A,\lambda} \cdot \varepsilon_{A,\lambda} \cdot [A] \cdot G_\lambda = k_{A,\lambda} \cdot [A] \cdot G_\lambda \tag{2}$$

where k_λ is the kinetic constant (mJ^{-1} cm^2) at the specific wavelength with respect to the concentration of the reactant and the irradiance. On the other hand, the kinetic constants for the DCF photolysis at different wavelengths and the dark reactions were obtained from this work's experimental data.

3. Results and discussion

3.1. Lamps characterisation

The irradiance values of the lamps evaluated through chemical

Table 1
Lamps' characterisation through the chemical actinometry and the ILT radiometer.

Lamp wavelength (nm)	Irradiance from actinometry (mW cm^{-2})	Max. Irradiance from ILT (mW cm^{-2})	Current (A)	Total Electric Power (W)
265	21.98 ± 0.43	26.07	0.75	36.14
285	31.18 ± 0.06	39.44	0.97	46.56
310	27.62 ± 0.61	29.59	0.64	30.72

actinometry and the ILT radiometer are shown in Table 1.

The values from chemical actinometry were considered for the rest of the study. Indeed, actinometry took into consideration the refractions occurring in water and the loss due to the quartz tube, while the radiometer measured the value in the air. Each lamp was also characterised at different intensities by regulating the voltage through a power supply. A linear relationship was confirmed with the current and the irradiation versus lamp intensity (Appendix A).

3.2. Diclofenac degradation

3.2.1. Molar absorption coefficient of the diclofenac and the oxidants

The molar absorption coefficient was measured using the gradient concentration methods and the Lamber-Beer law, Eq. (3).

$$A = \varepsilon_\lambda \, b \, C \tag{3}$$

where A is the absorbance measured through the spectrophotometer, C is the molar concentration (M), and b is the path lengths of the quartz cuvette (1 cm). The pH conditions were measured for the solutions with 20 mg L^{-1} of DCF, 20 mg L^{-1} of H_2O_2, and 20 mg L^{-1} of FC. They were respectively 7.2, 6.5, and 8.5, and no further adjustment was made. The absorption spectra of the compound and the oxidants compared to the lamp's emission spectra are shown in Fig. 2.

Finally, the values at the specific wavelengths of interest are reported in Table 2.

3.2.2. Degradation at different wavelengths

DCF degradation followed in all cases a pseudo-first-order kinetic, which can be described as a function of time, Eq. (4), or UV fluence, Eq. (5), where the mass balance was considered to adjust the kinetics based on the active volume of the reactor over the total volume, to account for the actual photoreactor contact time and have system-independent results comparable with other studies.

$$\ln\left(\frac{C}{C_0}\right) = -k \cdot t \cdot \frac{V_R}{V_T} \tag{4}$$

$$\ln\left(\frac{C}{C_0}\right) = -k^{'} \cdot UV_{fluence} \tag{5}$$

where C_0 is the initial concentration of diclofenac in the system, C is the concentration at a specific time t (min) inside the reactor, k is the time-based kinetic constant (min^{-1}), k' is the UV fluence-based kinetic constant (mJ^{-1} cm^2), V_R is the active volume of the reactor (L), and V_T is the total volume (L). To note that the irradiance of the three lamps is different, as detailed in Table 1, and therefore the interest in both values for discussion.

Fig. 3 illustrates the degradation of DCF via direct photolysis, dark oxidation, UV/FC and UV/H_2O_2 with respect to the operation time and to the UV fluence in the active reactor. The experiments were performed in triplicate, where the average values are reported, and the error bars represent the standard deviation error among the repetitions.

Table 2
The molar absorption coefficient for DCF (pH 7.2), HOCl/OCl^- (pH 8.5), and H_2O_2 (pH 6.5) measured in this study at the wavelength of interest.

Compound/Oxidant	ε, M^{-1} cm^{-1}			
	254 nm	265 nm	285 nm	310 nm
Diclofenac	4740.14	7126.11	7157.93	1113.46
Hypochlorous acid and hypochlorite ion	71.49	173.86	388.75	300.52
Hydrogen peroxide	20.76	8.58	4.24	0.62

A removal dependency on the wavelength was found in agreement with the absorption coefficient of the diclofenac and the oxidant employed, which are shown in Table 2. We can observe that the UV fluence-based constants for 265 and 285 nm have similar values during UV photolysis, but it is lower for 310 nm. On the other hand, a higher k' value can be observed for 285 nm/FC, while 265 nm had the highest k' value in combination with H_2O_2. This follows the wavelength dependency of the oxidant's activation; hypochlorite ion has a higher absorbance value and molar absorption coefficient at 285 nm, while H_2O_2 has a higher absorption at lower wavelengths. In all cases, the lamp at 310 nm had the lowest degradation impact in agreement with the diclofenac absorption at 310 nm, which was the smallest. However, the best result with the latter was achieved with FC since a good activation of the oxidant was possible.

In order to quantify the synergistic effect by coupling the oxidation process with the photolysis, the synergy factor was measured in each case, as shown in Eq. (6) and represented in Fig. 4, where the error was measured through the propagation of uncertainty among the experimental measurements.

$$F_S = \frac{k_{UV/oxidant}}{k_{UV} + k_{oxidant}} \tag{6}$$

The dashed line corresponds to the line of "no-synergy", where the final k is equal to the sum of each single treatment. By adding chlorine, the highest synergy was reached by the 285 and 310 nm lamp, while with hydrogen peroxide, 265 followed by 285 nm were the wavelengths with the highest synergistic factor, in agreement with the wavelength dependency of the contaminant and the oxidant's activation. In all cases, a synergistic effect was reached when coupling the UV treatment with the oxidants, except for the 310 nm/H_2O_2. In the latter, the synergy was not obtained since the absorption of H_2O_2 at 310 nm is nearly null, and therefore the 310/H_2O_2 combination essentially worked like the 310 nm treatment.

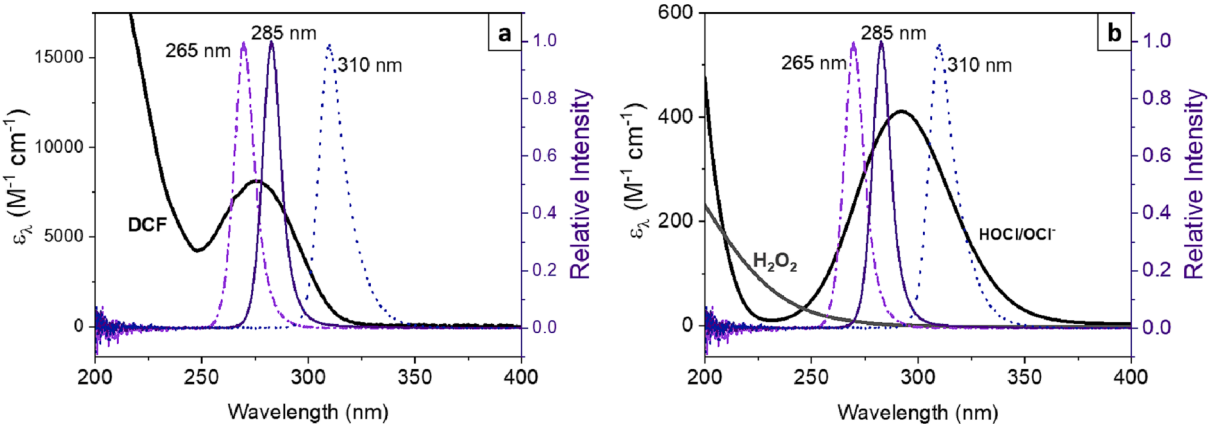

Fig. 2. The absorbance of DCF (pH 7.2) (a), HOCl/OCl^- (pH 8.5), and H_2O_2 (pH 6.5) (b).

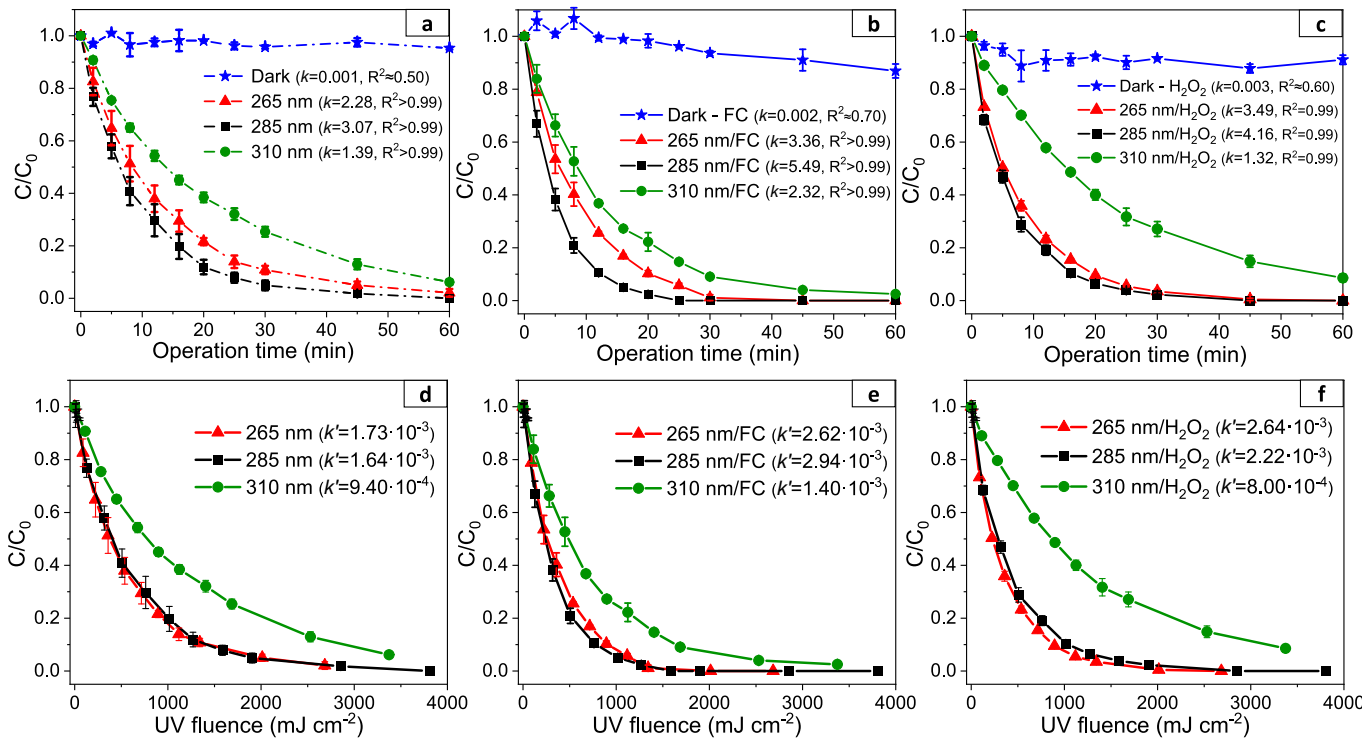

Fig. 3. The degradation of DCF (20 mg L^{-1}) versus time and UV fluence by photolysis alone (a, d), UV/FC oxidation with 20 mg L^{-1} of FC (b, e), and UV/H_2O_2 oxidation with 20 mg L^{-1} of H_2O_2 (c, f), where k is the time-based kinetic constant (expressed in min^{-1}) and k' is the UV fluence-based kinetic constant (expressed in mJ^{-1} cm^2).

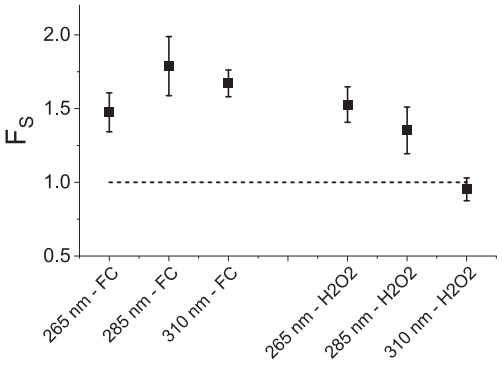

Fig. 4. The extent of synergy in the UV-LED/FC and UV-LED/H_2O_2 treatment.

3.2.3. Rigorous kinetic model

To describe the DCF degradation by UV irradiation-driven AOPs as a function of wavelength, a rigorous kinetic model is proposed for UV/H_2O_2 (Table 3) and UV/FC (Table 4), where the mechanisms suggested were the best compromise between the number of reactions and the robustness of the result.

Through the resolution of the mass balances of the different species, assuming the MSSA of the hydroxyl and chlorine radicals, and minimising the NRMSE between the experimental and predicted data, the kinetic constants to estimate k_{HO} and k_{Cl}, corresponding to reactions *R4a* and to *R7b,* were evaluated. Details of the derivation of the model and the calculation of the constants can be found in Appendix H and Appendix I of the Supplementary Information for the UV/H_2O_2 and UV/FC treatment, respectively.

The value obtained for the second-order rate constant for HO• with DCF, k_{HO}, was $9.12 \cdot 10^9$ M^{-1} s^{-1}, which is in agreement with the values reported in the literature, 7.6–$9.1 \cdot 10^9$ [20], $9.29 \cdot 10^9$ [29], and $1.36 \cdot 10^{10}$ [30] M^{-1} s^{-1}. On the other hand, during the UV/FC process, among

Table 3
Proposed mechanism for the UV/H_2O_2 treatment.

#	Reaction	Rate	Kinetic constant	Unit	Ref
(R1a)	$DCF + h\nu \rightarrow products$	$k_{fotolisis,\lambda}[DCF]G_\lambda$	$k_{F,265} = 1.73 \cdot 10^{-3}$ $k_{F,285} = 1.64 \cdot 10^{-3}$ $k_{F,310} = 9.40 \cdot 10^{-4}$	$mJ^{-1}cm^2$	This work
(R2a)	$DCF + H_2O_2 \rightarrow products$	$k_{perox}[DCF][H_2O_2]$	$k_{perox} = 0.061$	$M^{-1}s^{-1}$	This work
(R3a)	$H_2O_2 + h\nu \rightarrow 2HO\bullet$	$k_{f,H2O2}[H_2O_2]G_\lambda$	$k_{fH2O2,265} = 9.52 \cdot 10^{-6}$ $k_{fH2O2,285} = 5.06 \cdot 10^{-6}$ $k_{fH2O2,310} = 8.08 \cdot 10^{-7}$	$mJ^{-1}cm^2$	Φ_λ, from [26] ε_λ, from this work
(R4a)	$DCF + HO\bullet \rightarrow products$	$k_{HO}[DCF][HO\bullet]$	To estimate	$M^{-1}s^{-1}$	Determined in this work
(R5a)	$2HO\bullet \rightarrow H_2O_2$	$k_{Recomb}[HO\bullet]^2$	$k_{Recomb} = 5.5 \cdot 10^9$	$M^{-1}s^{-1}$	[26]
(R6a)	$H_2O_2 + HO\bullet \rightarrow HO_2\bullet + H_2O$	$k_1[H_2O_2][HO\bullet]$	$k_1 = 2.7 \cdot 10^7$	$M^{-1}s^{-1}$	[27]
(R7a)	$H_2O_2 + HO_2\bullet \rightarrow HO\bullet + H_2O + O_2$	$k_2[H_2O_2][HO_2\bullet]$	$k_2 = 3.7$	$M^{-1}s^{-1}$	[27]

Table 4
Proposed mechanism for the UV/FC treatment.

#	Reaction	Rate	Kinetic constant	Unit	Ref
(R1b)	$HOCl \rightleftarrows OCl^- + H^+$		$pKa^* = 7.5$		[28]
(R2b)	$HOCl + h\nu \rightarrow HO\bullet + Cl\bullet$	$k_{HOCl,\lambda}[HOCl]G_\lambda$	$k_{HOCl,268} = 7.60{\cdot}10^{-5}$ $k_{HOCl,282} = 6.25{\cdot}10^{-5}$ $k_{HOCl,301} = 6.29{\cdot}10^{-5}$.	$mJ^{-1}cm^2$	[26]
(R3b)	$OCl^- + h\nu \rightarrow O^-\bullet + Cl\bullet$	$k_{OCl-,\lambda}[OCl^-]G_\lambda$	$k_{OCl-,265} = 3.75 \cdot 10^{-4}$ $k_{OCl-,285} = 7.61{\cdot}10^{-4}$ $k_{OCl-,310} = 6.01 \cdot 10^{-4}$	$mJ^{-1}cm^2$	Φ_λ, from [26] ε_λ, from this work
(R4b)	$DCF + HO\bullet \rightarrow products$	$k_{HO}[DCF][HO\bullet]$	k_{HO} calculated from UV/H_2O_2 kinetic	$M^{-1}s^{-1}$	This work
(R5b)	$HO\bullet + HOCl \rightarrow ClO\bullet + H_2O$	$k_{HO,A}[HO\bullet][HOCl]$	$k_{HO,A} = 2.0{\cdot}10^9$	$M^{-1}s^{-1}$	[17]
(R6b)	$HO\bullet + OCl^- \rightarrow ClO\bullet + OH^-$	$k_{HO,B}[HO\bullet][OCl^-]$	$k_{HO,B} = 8.8{\cdot}10^9$	$M^{-1}s^{-1}$	[17]
(R7b)	$DCF + Cl\bullet \rightarrow products$	$k_{Cl}[DCF][Cl\bullet]$	To estimate	$M^{-1}s^{-1}$	Determined in this work
(R8b)	$DCF + HOCl \rightarrow products$	$k_{d,HOCl}[DCF][HOCl]$	$k_{d,HOCl} = 0.0077$	$M^{-1}s^{-1}$	This work
(R9b)	$Cl\bullet + HOCl \rightarrow Cl^- + ClO\bullet + H^+$.	$k_{Excess,\ A}[Cl\bullet][HOCl]$	$k_{Excess,\ A} = 3.0{\cdot}10^9$	$M^{-1}s^{-1}$	[17]
(R10b)	$Cl\bullet + OCl^- \rightarrow Cl^- + ClO\bullet$	$k_{Excess,\ B}[Cl\bullet][OCl^-]$	$k_{Excess,\ B} = 8.2{\cdot}10^9$	$M^{-1}s^{-1}$	[17]
(R11b)	$DCF + OCl^- \rightarrow products$	$k_{d,OCl^-}[DCF][OCl^-]$	$k_{d,OCl-} = 0.0772$	$M^{-1}s^{-1}$	This work
(R12b)	$DCF + h\nu \rightarrow products$	$k_{fotolisis,\lambda}[DCF]G_\lambda$	$k_{F,265} = 1.73{\cdot}10^{-3}$ $k_{F,285} = 1.64{\cdot}10^{-3}$ $k_{F,310} = 9.40{\cdot}10^{-4}$	$mJ^{-1}cm^2$	This work

the reactive chlorine species, Cl•, Cl_2^{-}• and ClO•, Cl• can be considered the most reactive for the diclofenac degradation [31]. The second-order rate constant for Cl• with DCF was estimated to be $1.30 \cdot 10^{10}$ M^{-1} s^{-1}, which is also in agreement with the value in literature of $3.77 \cdot 10^{10}$ M^{-1} s^{-1} [32] and in the range of other similar contaminants such as carbamazepine $5.6 \cdot 10^{10}$ M^{-1} s^{-1} [33] and N,N-diethyl-m-toluamide (DEET), $6.4 \cdot 10^9$ M^{-1} s^{-1} [34]. The model predictions based on $k_{HO} = 9.12 \cdot 10^9$ M^{-1} s^{-1} and $k_{Cl} = 1.30 \cdot 10^{10}$ M^{-1} s^{-1} are shown in Fig. 5, wherein the x-axis represents the photoreactor contact time, which is the operation time corrected with the active volume.

The model adequately fits the experimental data of the DCF degradation and the consumption of the reagents. Therefore, it can be considered that the degradation mechanisms are satisfactorily described by the reactions in Table 3 and Table 4, which can be used to extrapolate data at other conditions and different wavelengths.

3.2.4. Degradation at different intensities

A unique characteristic of the LEDs is the possibility of regulating

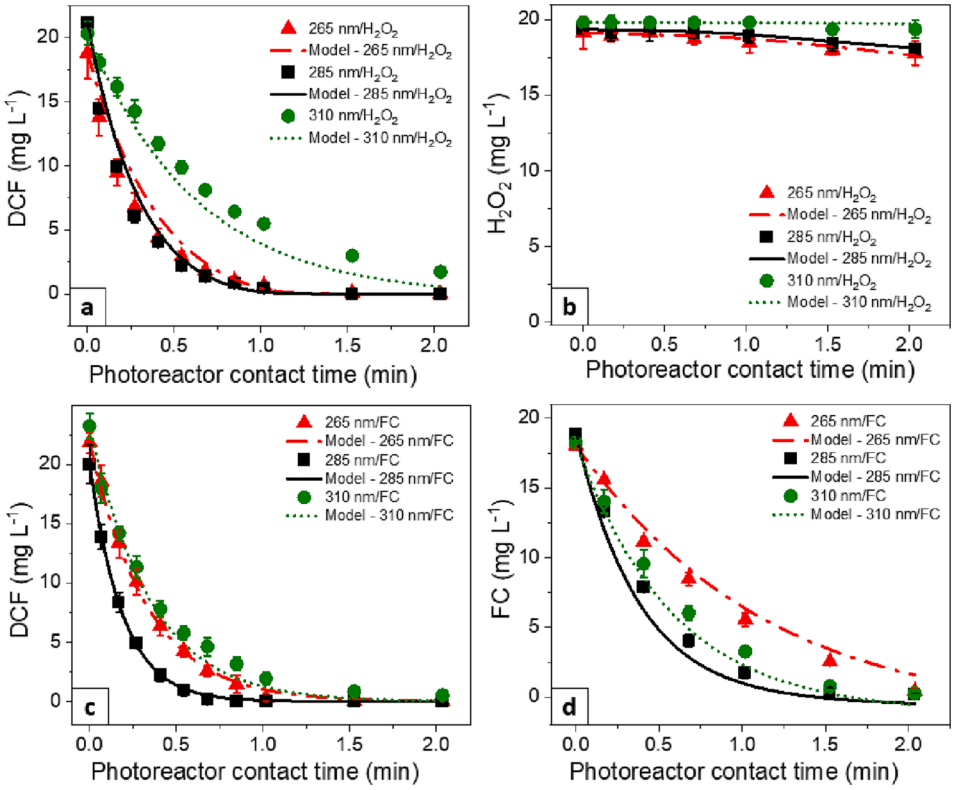

Fig. 5. Correlation between experimental data for diclofenac, hydrogen peroxide, and free chlorine (red triangles, black squares, and green dots for 265, 285 and 310 nm, respectively) and model predictions (red dashed-dotted, black solid, and green dotted lines for 265, 285 and 310 nm, respectively) during UV/H_2O_2 (a and b) and UV/FC (c and d) treatment.

their intensities. Through a digital input in Volts (0–10 V), it was possible to work at different irradiation levels and evaluate the impact on the oxidants' activation other than the direct photolysis degradation of the compound. The experiments were carried out at 25%, 50% and 75% of the total intensity of the 265 and 285 nm lamps since they exhibited the best results for DCF degradation.

Fig. 6 shows the time-based constants for the two lamps as a function of the lamp intensity. A linear correlation passing through the origin was found in all cases with a high correlation coefficient R^2.

Therefore, according to the second law of photochemistry [35], at a given wavelength, the rate of a photochemical reaction is proportional to the absorbed photon flux.

3.2.5. Dual-wavelength UV-LEDs

The effect of dual-wavelength UV photolysis on the decomposition of the contaminant and the oxidant was investigated for the 265 nm and 285 nm wavelengths. In Fig. 1, lamp 2 was added to the setup employed to investigate the potential dual-wavelength synergy. The irradiance of the two lamps irradiating in parallel was measured through chemical actinometry and compared to the sum of the irradiance of each lamp measured singularly. The two values were very close, respectively, 55.42 ± 1.60 mW cm^{-2} and 53.16 ± 0.43 mW cm^{-2}, showing that the lamps at those positions did not generate extra refractions due to the opposite lamp reflectors.

Fig. 7a shows the comparison among the "simulated" time-based constants, measured as the sum of the k evaluated for each lamp, and the "observed" (experimental) value where both wavelengths were irradiated at the same time. The experiments were also carried out for UV/FC and UV/H_2O_2 processes. The "simulated" and "observed" UV fluence-based constants, k', were not reported since they showed similar results.

In the case of photolysis alone, the observed value was slightly greater than the simulated one, while an opposite result was noticed during UV/FC and UV/H_2O_2 treatment. However, in all cases, the difference was very small considering the experimental error, which resulted from the repetitions of two sets of experiments in the case of the "observed" values, and calculated through the uncertainty propagation for the simulated ones. In Fig. 7b, the synergy factors for the three cases were also reported. Finally, a one-way ANOVA analysis was performed to evaluate the significance level (p) of the null hypothesis "all means are equal". The p-values were measured through the Minitab Software and were all above 0.05: 0.054, 0.061, and 0.068, respectively, for UV alone, UV/FC and UV/H_2O_2. Therefore, the differences between the values are not statistically significant since there is not enough evidence to reject the null hypothesis. In conclusion, this study has shown that the dual-wavelength system did not exhibit any remarkable synergy for the DCF degradation, and the observed removal can be attributed to the cumulative effect of the photons generated by both lamps. In agreement with the second law of photochemistry, as long as the wavelength is such that the photon energy is above the threshold for excitation, the photochemical rate is proportional to the absorbed photon flux [35]. This finding is consistent with Popova et al. [36] work, which investigated bisphenol A degradation using various wavelength combinations (222 + 282, 222 + 365, and 282 + 365 nm) and oxidants (potassium persulfate and hydrogen peroxide), and no synergy was observed. In contrast, Gao et al. [16] reported a statistically significant synergistic effect ($p < 0.05$) in the degradation of iopamidol using a dual-wavelength system (265 nm + 280 nm, each lamp at 50% intensity) through direct photolysis and UV/chlorine oxidation. Therefore, it is important to note that different micropollutants could lead to different results as they will exhibit different molar absorption coefficients. The synergy in the direct photolysis of iopamidol was explained as an enhancement of the number of photons between 265 and 280 nm, which potentially induced an increase in the rate to reach the excited state. At the same time, the synergy in UV/FC was also supported by the promotion of the photolysis of chlorine and the enhancement in reactive radicals' production. While synergy gained interest for disinfection purposes [37–39], to the best of the authors' knowledge, no other studies evaluated the extent of synergy in removing chemical compounds. Consequently, more studies are needed to clarify whether synergy might be significant during chemical degradation, the dependency on the micropollutant, and the mechanisms involved.

3.2.6. Energy consumption

The electrical energy per order (EEO) was evaluated for all the UV-LED processes to identify the overall energy consumption. EEO is defined as the electric energy in kWh required to reduce the concentration of a contaminant by one order of magnitude (90% removal) in 1 m^3 of water, and it is measured in batch operations according to Eq. (7) [40].

$$EEO_{UV} = \frac{P \cdot t}{V \cdot log\left(\frac{C_0}{C}\right)} \tag{7}$$

where P is the rated power or energy input (kW) of the lamp system, V (m^3) is the volume of water treated in the photoreactor contact time t (h). By converting the time in minutes and the volume in litres and considering a pseudo first-order kinetic where $\log(C_0/C)$ can be re-written as a function of the time-based kinetic constant, then Eq. (7) can be re-formulated in Eq. (8).

$$EEO_{UV} = \frac{1000 \cdot P(kW) \cdot t(min)}{V(L) \cdot 0.4343 \cdot k\left(min^{-1}\right) \cdot t(min) \cdot 60} = \frac{38.38 \cdot P}{V \cdot k} \tag{8}$$

During the UV/FC and UV/H_2O_2 treatment, the equivalent electrical energy of the oxidant was also considered, accordingly to Eq. (9) and Eq.

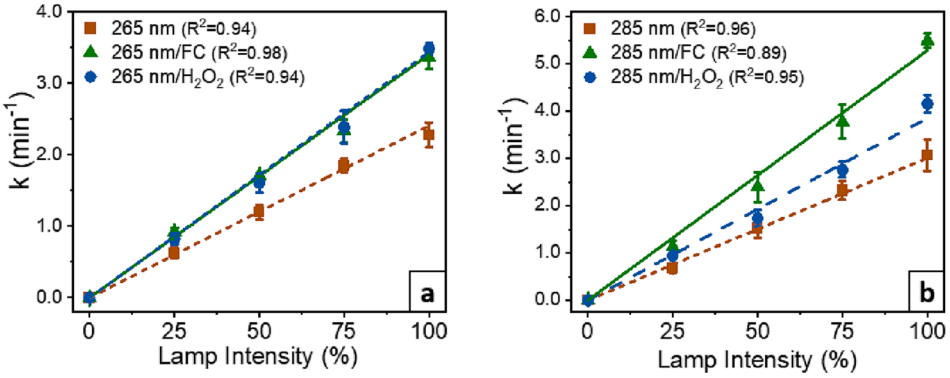

Fig. 6. Linear correlation between the time-based constants and the lamp intensity for the lamps at 265 nm (a) and 285 nm (b) for UV alone (brown squares), UV/FC (green triangles), and UV/H_2O_2 (blue dots). (For interpretation of the references to colour in this figure legend, the reader is referred to the web version of this article.)

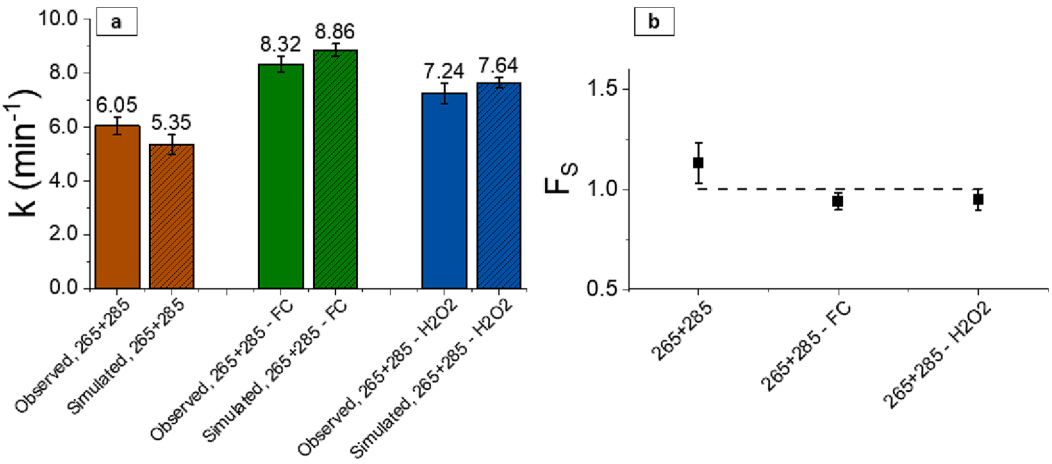

Fig. 7. Time-based constants "observed" and "simulated" (a) and the extent of synergy (b) during the dual-wavelength irradiation.

(10).

$$EEO_{oxidant} = Eq_{oxidant} \cdot \frac{[oxidant]_0}{log\left(\frac{C_0}{C}\right)} \quad (9)$$

$$EEO_{total} = EEO_{UV} + EEO_{oxidant} \quad (10)$$

where $Eq_{oxidant}$ is the equivalent electric energy consumption to produce a milligram of oxidant, which is $1.16 \cdot 10^{-5}$ and $1.08 \cdot 10^{-5}$ kWh mg^{-1} for chlorine and hydrogen peroxide, respectively [33,41], and $[oxidant]_0$ is the initial concentration of oxidant added in mg m^{-3}. In this case, log (C_0/C) can be directly considered as one which corresponds to the reduction of one order of magnitude of the contaminant.

Table 5 reports the electrical energy consumption at different wavelengths in the case of direct photolysis, UV/FC and UV/H_2O_2. The electrical energy consumption at different intensities was not reported as similar values of their corresponding 100% intensity were obtained.

Despite the higher degradation rate during the UV-driven AOPs, the electricity demand of the overall process is similar to photolysis alone due to the oxidant demand. Regardless of the lower total electric power and the lower current of the 310 nm lamp, the total EEO resulted higher than the other cases and, therefore, the least performing. The other two lamps gave comparable results during photolysis, but combined with chlorine, 285 nm performed the best, while with H_2O_2, 265 nm followed by 285 nm outstood.

Table 5
The electrical energy consumption of DCF degradation during different photolysis processes.

	Oxidant dosage	$EEO_{oxidant}$	EEO_{UV} @ 100%	EEO_{total} @ 100%
	(mg L^{-1})		(kWh m^{-3} $order^{-1}$)	
UV				
265 nm	–	0.00	0.61 ± 0.05	0.61 ± 0.05
285 nm	–	0.00	0.58 ± 0.06	0.58 ± 0.06
310 nm	–	0.00	0.85 ± 0.05	0.85 ± 0.05
265 + 285 nm	–	0.00	0.52 ± 0.03	0.52 ± 0.03
UV/FC				
265 nm	20	0.23	0.41 ± 0.02	0.64 ± 0.02
285 nm	20	0.23	0.33 ± 0.01	0.56 ± 0.01
310 nm	20	0.23	0.51 ± 0.00	0.74 ± 0.00
265 + 285 nm	20	0.23	0.38 ± 0.01	0.61 ± 0.01
UV/H_2O_2				
265 nm	20	0.22	0.40 ± 0.01	0.61 ± 0.01
285 nm	20	0.22	0.43 ± 0.02	0.65 ± 0.02
310 nm	20	0.22	0.89 ± 0.05	1.11 ± 0.05
265 + 285 nm	20	0.22	0.44 ± 0.02	0.66 ± 0.02

3.2.7. Mineralisation of DCF and phytotoxicity

The mineralisation and phytotoxicity tests were performed after the different treatments and are shown in Table 6.

While after each treatment, DCF was almost completely removed, DOC decreased only partially by 20–30%, regardless of the degradation process used. Something similar was observed by Peng et al. [42], who explored the DCF degradation by UV-activated peroxymonosulfate after 2 h and by Fischer et al. [43] after 18 h of UV-A irradiation. Also, Leydy Katherine Ardila et al. [44] reported insignificant mineralisation after 30 min of direct photolysis or TiO_2-induced hydroxylation. Even if there are other studies that reached a high degree of mineralisation when longer irradiation periods and a higher amount of oxidants were employed [44], it can be concluded that the degradation of DCF by-products is more recalcitrant than DCF itself, and it needs longer exposure time to completely remove them if complete removal is possible through photolysis and oxidation.

Regardless of the treatment, a visible yellowish colour appeared in all cases during the degradation of diclofenac. According to Keen et al. [45] and Iovino et al. [46], the colour could be addressed to the formation of dimers, which are stable forms to UV irradiation. Therefore, in agreement with the DOC analysis, only a small part of the parent compound degrades to eventually form H_2O, HCl and CO_2, and the rest go through condensation and form these stable dimers, preventing further pollutant degradation. Nevertheless, the use of AOPs might help further the degradation of the by-products. However, even if Li et al. [17] highlighted slightly different by-products after UV/FC, dimerisation still occurs. On the other hand, Lekkerkerker-Teunissen et al. [18] suggested that the influence of hydrogen peroxide in the degradation by-product path may be minimal and follow the same pattern as the UV direct photolysis.

Regarding the phytotoxicity tests, a sample with a germination index

Table 6
DOC removal and germination index (GI) after treatment.

Treatment	DOC (mg L^{-1})	DOC removal (%)	GI (%) for radish	GI (%) for tomato
DCF in water, 20 mg L^{-1}	10.95 ± 0.11	–	39.15 ± 5.53	23.42 ± 5.16
265 nm, operation time: 60 min	8.84 ± 0.25	19.26 ± 2.24	57.56 ± 4.16	36.05 ± 4.20
285 nm, operation time: 60 min	7.40 ± 0.35	22.39 ± 3.18	60.82 ± 7.07	39.56 ± 7.75
265 nm/H_2O_2, operation time: 60 min	8.29 ± 0.20	24.29 ± 1.87	71.60 ± 9.11	49.46 ± 9.98
285 nm/FC, operation time: 60 min	8.70 ± 0.09	30.56 ± 0.78	58.65 ± 3.22	47.72 ± 2.26

below 70% is considered phytotoxic, while above 70% could be regarded as safe to release into the environment [24]. A sample of 20 mg L^{-1} of diclofenac alone in distilled water gave a GI value below 70% in both radish and tomato seeds, where the tomato seeds were the most affected by the presence of the pollutant in agreement with Ghanbari et al. [24], who found tomato to have a greater sensitivity to toxic effluents. After treatment, the GI values increased by around 20–30 percentage points in radish germination and 15–20 points in tomato plants. As expected, the treatments by UV direct photolysis alone, 265 nm or 285 nm, gave similar values, while among the oxidation processes, the H_2O_2 seems to lead to higher detoxification compared to FC, in particular for the radish seeds; however, the difference is almost nil if considering the experimental error.

In this investigation, the change in phytotoxicity was selected since there are scarce studies on it [47]. Majewska et al. [47] evaluated the impact of untreated diclofenac (32.7 mg L^{-1}) on the green alga *Chlamydomonas reinharditii,* and it was found that DCF was causing oxidative stress and photosynthesis inhibition. Another study was performed on *Chichorium intybus* seedlings irrigated with DCF solution (1 mg L^{-1}), showing a decrease in root biomass and an effect on chlorophyll biosynthesis but an increase in root length [48]. The phytotoxicity on *Lactuca sativa* was also investigated, but neither the initial DCF solution nor the treated solution was toxic [44]. Finally, the closest study was conducted by Naddeo et al. [49]. They evaluated the GI for *Lepidium sativum* (garden cress) but for a mixture of pharmaceuticals (DCF, amoxicillin, and carbamazepine with a DCF concentration of 2.5 mg L^{-1} in the mix) treated under ultrasonic irradiation. Surprisingly, the spiked WWTP effluent, compared to the non-spiked effluent, stimulated higher seed growth, explained by the added nutrient elements given by the low drug concentration; however, not all the experimental conditions led to a decrease in toxicity after the treatment. To note that the concentration of the other pharmaceuticals was higher than the one of DCF, which might have been less influential in the mixture. Moreover, Naddeo et al. [49] highlighted in the same study that the pharmaceutical mixture was severely toxic for the microalga *Pseudokirchneriella subcapitata*.

In this study, UV-based treatments were effective in decreasing phytotoxicity, although it is important to acknowledge that in numerous cases, including the present study, the toxicity of DCF was not reduced below the safe limit. Nevertheless, we should bear in mind that the actual concentrations of diclofenac in natural water systems are considerably lower than those examined in many experimental conditions.

Other investigations focused on the toxicity of diclofenac by-products towards *Vibrio fischeri, Vibrio quighaiensis*, *Photobacterium leiognathid*, *Daphnia similis*, and *Mus musculus* mice kidneys and livers. The toxicity towards bacteria generally shows increased toxicity due to unstable by-products followed by a toxicity decrease with further treatment [43,50]. Finally, untreated DCF was found to cause tumours in mice livers, while no adverse effect was found after DCF was treated by simulated solar-UV-A/ZnO/PPS [51]. Also, in another study [44], a solution of 20 mg L^{-1} of DCF resulted to likely cause the mortality of all *Daphnia similis* organisms, while direct photolysis and TiO_2-assisted photodegradation were capable of strongly reducing the toxicity.

During the treatment, a second peak in the HPLC spectra appeared during the photolysis reaction at a shorter retention time. This peak, also reported in other studies [45], is associated with a potentially toxic and unstable by-product, which explains the up-and-down toxicity behaviour towards the bacteria. It rapidly increased during the treatment, but after reaching a maximum, it decreased much more slowly than the increase (Appendix G in Supplementary Information). Therefore, for UV-based treatments to be effective, the treatment time has to be carefully selected to avoid the presence of more toxic and unstable by-products.

While it is not the focus of this work, in this regard, several studies have carefully identified the DCF degradation by-products using liquid chromatography-mass spectroscopy (LC-MS) often associated with the ecological structure activity relationship (ECOSAR) simulation, where the latter allows the estimation to aquatic organisms by using the structure activity relationships of the by-product. The research available extensively covers the by-products formed during UV [18,30,44], UV/H_2O_2 [18,30], UV/FC [17], and water chlorination [52]. In general, it can be concluded that predicted chronic ecotoxicity towards fish, daphnids and algae is reduced [44]; however, some intermediates possess higher toxicity than DCF itself [17]. The degradation paths in the three UV processes are similar; DCF first loses its first chlorine, followed by the second chlorine (being one of the two structures, the potential toxic by-product), and finally, in all cases, it forms dimers.

4. Conclusions

This work explored the application of 265, 285, and 310 nm LED emitters to remove diclofenac via photolysis alone (pH 7.2) and in combination with hydrogen peroxide (pH 6.5) or free chlorine (pH 8.5). The pseudo-first-order model described well the degradation of DCF, and a removal dependency on the wavelength was found in conformity with the absorption coefficient of the diclofenac and the oxidants. The highest DCF degradation constants were achieved for the lamps at 265 and 285 nm. A synergistic effect was reached when coupling the UV treatment with the oxidants; in particular, the highest synergistic factors were achieved for 285 and 310 nm with FC, and 265 followed by 285 nm with H_2O_2, following the absorption trend of the oxidants. Finally, no synergy was obtained with 310 nm/H_2O_2 since the absorption of the latter at that wavelength is nearly null. Despite the higher degradation by UV-LED driven AOPs than photolysis alone, the overall treatments have similar energy costs due to the energy consumed to produce the oxidants. The reaction mechanisms for UV/H_2O_2 and UV/FC were proposed, and a good fit between the experimental and simulated data was obtained with the estimated second-order kinetic constants $k_{HO} = 9.12 \cdot 10^9\ M^{-1}\ s^{-1}$ for HO• with DCF, and $k_{Cl} = 1.30 \cdot 10^{10}\ M^{-1}\ s^{-1}$ for Cl• with DCF. Studies at different intensities, performed at 265 and 285 nm, highlighted a linear correlation with the time-based degradation constants, which is important, given a desired removal, for selecting the residence time or the irradiation intensity inside the reactor. Furthermore, in this study, a dual-wavelength system (265 + 285 nm) alone and in combination with the oxidants was investigated, but no significant synergy ($p > 0.05$) was found. Regardless of the treatment, while the diclofenac was completely removed, the dissolved organic carbon decreased only partially by 20–30%. The formation of stable dimers explains the limited DOC removal, which is confirmed by the yellowish colour formed after each photolysis process and deserves additional attention as further treatment might need to be implemented to remove them. On the other hand, the phytotoxicity test revealed that the treated DCF solution was less toxic for radish and tomato seeds than untreated DCF. Whilst the germination index has remained below the safe phytotoxicity limit of 70%, UV-based treatments are generally effective in reducing toxicity. Nonetheless, careful selection of both time and irradiation intensity is necessary to prevent the presence of more toxic and unstable by-products. Overall, the results provide valuable evidence for the application of UV-B and UV-C LED emitters in water treatment plants, where factors like tuneable wavelength, instant on–off, and adjustable intensity can be positively exploited.

Further work related to these results should focus on real wastewater scenarios to judge the practical applicability of the UV LED lamps and explore the potential environmental impacts of the three processes through LCA analysis to evaluate the technology hotspots and areas of improvement.

Declaration of Competing Interest

The authors declare that they have no known competing financial interests or personal relationships that could have appeared to influence the work reported in this paper.

Data availability

Data will be made available on request.

Acknowledgement

The authors acknowledge the financial support of the European Union's Horizon 2020 research and innovation programme in the frame of REWATERGY, Sustainable Reactor Engineering for Applications on the Water-Energy Nexus, MSCA-ITN-EID Project N. 812574. R. Pizzichetti would also like to thank Anna Hogan for her help with the HPLC.

Appendix A. Supplementary data

Supplementary data to this article can be found online at https://doi.org/10.1016/j.cej.2023.144520.

References

[1] C.M. Villanueva, M. Kogevinas, S. Cordier, M.R. Templeton, R. Vermeulen, J. R. Nuckols, M.J. Nieuwenhuijsen, P. Levallois, Assessing exposure and health consequences of chemicals in drinking water: Current state of knowledge and research needs, Environ. Health Perspect. 122 (2014) 213–221, https://doi.org/10.1289/ehp.1206229.

[2] A. Ruhí, V. Acuña, D. Barceló, B. Huerta, J.R. Mor, S. Rodríguez-Mozaz, S. Sabater, Bioaccumulation and trophic magnification of pharmaceuticals and endocrine disruptors in a Mediterranean river food web, Sci. Total Environ. 540 (2016) 250–259, https://doi.org/10.1016/j.scitotenv.2015.06.009.

[3] O.M. Rodriguez-Narvaez, J.M. Peralta-Hernandez, A. Goonetilleke, E.R. Bandala, Treatment technologies for emerging contaminants in water: a review, Chem. Eng. J. 323 (2017) 361–380, https://doi.org/10.1016/j.cej.2017.04.106.

[4] L. Rizzo, S. Malato, D. Antakyali, V.G. Beretsou, M.B. Đolić, W. Gernjak, E. Heath, I. Ivancev-Tumbas, P. Karaolia, A.R. Lado Ribeiro, G. Mascolo, C.S. McArdell, H. Schaar, A.M.T. Silva, D. Fatta-Kassinos, Consolidated vs new advanced treatment methods for the removal of contaminants of emerging concern from urban wastewater, Sci. Total Environ. 655 (2019) 986–1008, https://doi.org/10.1016/j.scitotenv.2018.11.265.

[5] P.O. Ozuah, Mercury poisoning, Curr. Probl. Pediatr. 30 (2000) 91–99, https://doi.org/10.1067/mps.2000.104054.

[6] J.F.J.R. Pesqueira, J. Marugán, M.F.R. Pereira, A.M.T. Silva, Selecting the most environmentally friendly oxidant for UVC degradation of micropollutants in urban wastewater by assessing life cycle impacts: Hydrogen peroxide, peroxymonosulfate or persulfate? Sci. Total Environ. 808 (2022), 152050 https://doi.org/10.1016/j.scitotenv.2021.152050.

[7] W.L. Wang, Q.Y. Wu, Z.M. Li, Y. Lu, Y. Du, T. Wang, N. Huang, H.Y. Hu, Light-emitting diodes as an emerging UV source for UV/chlorine oxidation: Carbamazepine degradation and toxicity changes, Chem. Eng. J. 310 (2017) 148–156, https://doi.org/10.1016/j.cej.2016.10.097.

[8] G. Cerreta, M.A. Roccamante, P. Plaza-Bolaños, I. Oller, A. Aguera, S. Malato, L. Rizzo, Advanced treatment of urban wastewater by UV-C/free chlorine process: micro-pollutants removal and effect of UV-C radiation on trihalomethanes formation, Water Res. 169 (2020), 115220, https://doi.org/10.1016/j.watres.2019.115220.

[9] Y. Xiang, J. Fang, C. Shang, Kinetics and pathways of ibuprofen degradation by the UV/chlorine advanced oxidation process, Water Res. 90 (2016) 301–308, https://doi.org/10.1016/j.watres.2015.11.069.

[10] G. Matafonova, V. Batoev, Recent advances in application of UV light-emitting diodes for degrading organic pollutants in water through advanced oxidation processes: a review, Water Res. 132 (2018) 177–189, https://doi.org/10.1016/j.watres.2017.12.079.

[11] R. Yin, L. Ling, C. Shang, Wavelength-dependent chlorine photolysis and subsequent radical production using UV-LEDs as light sources, Water Res. 142 (2018) 452–458, https://doi.org/10.1016/j.watres.2018.06.018.

[12] J. DeLatt, M. Stefan, Advanced Oxidation Processes for Water Treatment, in: M. Stefan (Ed.), IWA Publ., 2018th ed., 2018.

[13] J.C.G. Sousa, A.R. Ribeiro, M.O. Barbosa, C. Ribeiro, M.E. Tiritan, M.F.R. Pereira, A.M.T. Silva, Monitoring of the 17 EU Watch List contaminants of emerging concern in the Ave and the Sousa Rivers, Sci. Total Environ. 649 (2019) 1083–1095, https://doi.org/10.1016/j.scitotenv.2018.08.309.

[14] L. Lonappan, S.K. Brar, R.K. Das, M. Verma, R.Y. Surampalli, Diclofenac and its transformation products: Environmental occurrence and toxicity - A review, Environ. Int. 96 (2016) 127–138, https://doi.org/10.1016/j.envint.2016.09.014.

[15] I. Alessandretti, C.V.T. Rigueto, M.T. Nazari, M. Rosseto, A. Dettmer, Removal of diclofenac from wastewater: a comprehensive review of detection, characteristics and tertiary treatment techniques, J. Environ. Chem. Eng. 9 (2021), https://doi.org/10.1016/j.jece.2021.106743.

[16] Z.C. Gao, Y.L. Lin, B. Xu, Y. Xia, C.Y. Hu, T.C. Cao, X.Y. Zou, N.Y. Gao, Evaluating iopamidol degradation performance and potential dual-wavelength synergy by UV-LED irradiation and UV-LED/chlorine treatment, Chem. Eng. J. 360 (2019) 806–816, https://doi.org/10.1016/j.cej.2018.12.022.

[17] Q. Li, C. Lai, J. Yu, J. Luo, J. Deng, G. Li, W. Chen, B. Li, G. Chen, Degradation of diclofenac sodium by the UV/chlorine process: Reaction mechanism, influencing factors and toxicity evaluation, J. Photochem. Photobiol. A Chem. 425 (2022), 113667, https://doi.org/10.1016/j.jphotochem.2021.113667.

[18] K. Lekkerkerker-Teunissen, M.J. Benotti, S.A. Snyder, H.C. Van Dijk, Transformation of atrazine, carbamazepine, diclofenac and sulfamethoxazole by low and medium pressure UV and UV/H2O2 treatment, Sep. Purif. Technol. 96 (2012) 33–43, https://doi.org/10.1016/j.seppur.2012.04.018.

[19] S. Mozia, D. Darowna, J. Przepiórski, A.W. Morawski, Evaluation of performance of hybrid photolysis-DCMD and photocatalysis-DCMD systems utilizing UV-C radiation for removal of diclofenac sodium salt from water, Polish, J Chem. Technol. 15 (2013) 51–60, https://doi.org/10.2478/pjct-2013-0010.

[20] Y. Huang, Y. Liu, M. Kong, E.G. Xu, S. Coffin, D. Schlenk, D.D. Dionysiou, Efficient degradation of cytotoxic contaminants of emerging concern by UV/H2O2, Environ. Sci. Water Res. Technol. 4 (2018) 1272–1281, https://doi.org/10.1039/c8ew00290h.

[21] J.R. Bolton, M.I. Stefan, P.S. Shaw, K.R. Lykke, Determination of the quantum yields of the potassium ferrioxalate and potassium iodide-iodate actinometers and a method for the calibration of radiometer detectors, J. Photochem. Photobiol. A Chem. 222 (2011) 166–169, https://doi.org/10.1016/j.jphotochem.2011.05.017.

[22] A.P. Uppinakudru, K. Reynolds, S. Stanley, C. Pablos, J. Marugán, Critical assessment of optical sensor parameters for the measurement of ultraviolet LED lamps, Measurement. 196 (2022), 111278, https://doi.org/10.1016/j.measurement.2022.111278.

[23] W. Li, R. Wu, J. Duan, C.P. Saint, D. Mulcahy, Overlooked effects of organic solvents from sample preparation on reaction constants of micropollutants in UV-based advanced oxidation processes, Chem. Eng. J. 313 (2017) 801–806, https://doi.org/10.1016/j.cej.2016.12.111.

[24] F. Ghanbari, Q. Wang, A. Hassani, S. Wacławek, J. Rodríguez-Chueca, K.Y.A. Lin, Electrochemical activation of peroxides for treatment of contaminated water with landfill leachate: efficacy, toxicity and biodegradability evaluation, Chemosphere. 279 (2021), 130610, https://doi.org/10.1016/j.chemosphere.2021.130610.

[25] C. Casado, J. Moreno-SanSegundo, I. De la Obra, B. Esteban García, J.A. Sánchez Pérez, J. Marugán, Mechanistic modelling of wastewater disinfection by the photo-Fenton process at circumneutral pH, Chem. Eng. J. 403 (2021), 126335, https://doi.org/10.1016/j.cej.2020.126335.

[26] S.R. Sarathy, M.M. Bazri, M. Mohseni, Modeling the transformation of chromophoric natural organic matter during UV/H2O2 advanced oxidation, J. Environ. Eng. 137 (2011) 903–912, https://doi.org/10.1061/(asce)ee.1943-7870.0000390.

[27] C.-H. Liao, M.D. Gurol, Chemical oxidation by photolytic, Environ. Sci. Technol. 29 (1995) 3007–3014.

[28] Y. Feng, D.W. Smith, J.R. Bolton, Photolysis of aqueous free chlorine species (HOCl and OCl-) with 254 nm ultraviolet light, J. Environ. Eng. Sci. 6 (2007) 277–284, https://doi.org/10.1139/S06-052.

[29] H. Yu, E. Nie, J. Xu, S. Yan, W.J. Cooper, W. Song, Degradation of diclofenac by advanced oxidation and reduction processes: kinetic studies, degradation pathways and toxicity assessments, Water Res. 47 (2013) 1909–1918, https://doi.org/10.1016/j.watres.2013.01.016.

[30] S. Ledakowicz, E. Drozdek, T. Boruta, M. Foszpańczyk, M. Olak-Kucharczyk, R. Zyłła, M. Gmurek, Impact of hydrogen peroxide on the UVC photolysis of diclofenac and toxicity of the phototransformation products, Int. J. Photoenergy. 1155 (2019) 1086704, https://doi.org/10.1155/2019/1086704.

[31] K. Guo, Z. Wu, C. Chen, J. Fang, UV/chlorine process: an efficient advanced oxidation process with multiple radicals and functions in water treatment, Acc. Chem. Res. 55 (2022) 286–297, https://doi.org/10.1021/acs.accounts.1c00269.

[32] Y. Lei, S. Cheng, N. Luo, X. Yang, T. An, Rate constants and mechanisms of the reactions of Cl• and Cl2•- with trace organic contaminants, Environ. Sci. Technol. 53 (2019) 11170–11182, https://doi.org/10.1021/acs.est.9b02462.

[33] W.L. Wang, Q.Y. Wu, N. Huang, T. Wang, H.Y. Hu, Synergistic effect between UV and chlorine (UV/chlorine) on the degradation of carbamazepine: influence factors and radical species, Water Res. 98 (2016) 190–198, https://doi.org/10.1016/j.watres.2016.04.015.

[34] P. Sun, W.N. Lee, R. Zhang, C.H. Huang, Degradation of DEET and caffeine under UV/Chlorine and simulated sunlight/Chlorine conditions, Environ. Sci. Technol. 50 (2016) 13265–13273, https://doi.org/10.1021/acs.est.6b02287.

[35] J.R. Bolton, I. Mayor-Smith, K.G. Linden, Rethinking the concepts of fluence (UV dose) and fluence rate: the importance of photon-based units - a systemic review, Photochem. Photobiol. 91 (2015) 1252–1262, https://doi.org/10.1111/php.12512.

[36] S.A. Popova, G.G. Matafonova, V.B. Batoev, Dual-wavelength UV degradation of bisphenol A and bezafibrate in aqueous solution using excilamps (222, 282 nm) and LED (365 nm): yes or no synergy? J. Environ. Sci. Heal. - Part A. 58 (2023) 39–52, https://doi.org/10.1080/10934529.2023.2172270.

[37] S.E. Beck, H. Ryu, L.A. Boczek, J.L. Cashdollar, K.M. Jeanis, J.S. Rosenblum, O. R. Lawal, K.G. Linden, Evaluating UV-C LED disinfection performance and investigating potential dual-wavelength synergy, Water Res. 109 (2017) 207–216, https://doi.org/10.1016/j.watres.2016.11.024.

[38] P.O. Nyangaresi, Y. Qin, G. Chen, B. Zhang, Y. Lu, L. Shen, Effects of single and combined UV-LEDs on inactivation and subsequent reactivation of E. coli in water disinfection, Water Res. 147 (2018) 331–341, https://doi.org/10.1016/j.watres.2018.10.014.

[39] Y. Kebbi, A.I. Muhammad, A.S. Sant'Ana, L. do Prado-Silva, D. Liu, T. Ding, Recent advances on the application of UV-LED technology for microbial inactivation: progress and mechanism, Compr. Rev. Food Sci. Food Saf. 19 (6) (2020) 3501–3527.

[40] J.R. Bolton, K.G. Bircher, W. Tumas, C.A. Tolman, Figures-of-merit for the technical development and application of advanced oxidation technologies for both electric- and solar-driven systems, Pure Appl. Chem. 73 (2001) 627–637, https://doi.org/10.1351/pac200173040627.
[41] Y. Xiao, L. Zhang, J. Yue, R.D. Webster, T.T. Lim, Kinetic modeling and energy efficiency of UV/H2O2 treatment of iodinated trihalomethanes, Water Res. 75 (2015) 259–269, https://doi.org/10.1016/j.watres.2015.02.044.
[42] Y. Peng, H. Shi, Z. Wang, Y. Fu, Y. Liu, Kinetics and reaction mechanism of photochemical degradation of diclofenac by UV-activated peroxymonosulfate, RSC Adv. 11 (2021) 6804–6817, https://doi.org/10.1039/d0ra10178h.
[43] K. Fischer, S. Sydow, J. Griebel, S. Naumov, C. Elsner, I. Thomas, A.A. Latif, A. Schulze, Enhanced removal and toxicity decline of diclofenac by combining uva treatment and adsorption of photoproducts to polyvinylidene difluoride, Polymers (Basel). 12 (2020) 1–15, https://doi.org/10.3390/polym12102340.
[44] P. Leydy Katherine Ardila, B.F. Da Silva, M. Spadoto, B. Clarice Maria Rispoli, E. B. Azevedo, Which route to take for diclofenac removal from water: Hydroxylation or direct photolysis? J. Photochem. Photobiol. A Chem. 382 (2019) https://doi.org/10.1016/j.jphotochem.2019.111879.
[45] O.S. Keen, E.M. Thurman, I. Ferrer, A.D. Dotson, K.G. Linden, Dimer formation during UV photolysis of diclofenac, Chemosphere. 93 (2013) 1948–1956, https://doi.org/10.1016/j.chemosphere.2013.06.079.
[46] P. Iovino, S. Chianese, S. Canzano, M. Prisciandaro, D. Musmarra, Photodegradation of diclofenac in wastewaters, Desalin. Water Treat. 61 (2017) 293–297, https://doi.org/10.5004/dwt.2016.11063.
[47] M. Majewska, D. Harshkova, M. Guściora, A. Aksmann, Phytotoxic activity of diclofenac: evaluation using a model green alga Chlamydomonas reinhardtii with atrazine as a reference substance, Chemosphere. 209 (2018) 989–997, https://doi.org/10.1016/j.chemosphere.2018.06.156.
[48] N.S. Podio, L. Bertrand, D.A. Wunderlin, A.N. Santiago, Assessment of phytotoxic effects, uptake and translocation of diclofenac in chicory (Cichorium intybus), Chemosphere. 241 (2020), 125057, https://doi.org/10.1016/j.chemosphere.2019.125057.
[49] V. Naddeo, S. Meriç, D. Kassinos, V. Belgiorno, M. Guida, Fate of pharmaceuticals in contaminated urban wastewater effluent under ultrasonic irradiation, Water Res. 43 (2009) 4019–4027, https://doi.org/10.1016/j.watres.2009.05.027.
[50] X. Lu, Y. Shao, N. Gao, J. Chen, Y. Zhang, H. Xiang, Y. Guo, Degradation of diclofenac by UV-activated persulfate process: Kinetic studies, degradation pathways and toxicity assessments, Ecotoxicol. Environ. Saf. 141 (2017) 139–147, https://doi.org/10.1016/j.ecoenv.2017.03.022.
[51] A. Smaali, M. Berkani, F. Merouane, V.T. Le, Y. Vasseghian, N. Rahim, M. Kouachi, Photocatalytic-persulfate- oxidation for diclofenac removal from aqueous solutions: modeling, optimization and biotoxicity test assessment, Chemosphere. 266 (2021), 129158, https://doi.org/10.1016/j.chemosphere.2020.129158.
[52] M. Soufan, M. Deborde, B. Legube, Aqueous chlorination of diclofenac: Kinetic study and transformation products identification, Water Res. 46 (2012) 3377–3386, https://doi.org/10.1016/j.watres.2012.03.056.